Annals of Biomedical Engineering, Vol. 24, pp. 537–543, 1996
Printed in the USA.

0090-6964/96 $10.50 + .00

A Comparison of Analytical Methods for the Study of Fractional Brownian Motion

RUSSELL FISCHER and METIN AKAY

Biomedical Engineering Department, Rutgers University, Piscataway, NJ

Abstract—Fractional Brownian motion (FBM) provides a useful model for many physical phenomena demonstrating long-term dependencies and $1/f$-type spectral behavior. In this model, only one parameter is necessary to describe the complexity of the data, H, the Hurst exponent. FBM is a nonstationary random function not well suited to traditional power spectral analysis however. In this paper we discuss alternative methods for the analysis of FBM, in the context of real-time biomedical signal processing. Regression-based methods utilizing the power spectral density (PSD), the discrete wavelet transform (DWT), and dispersive analysis (DA) are compared for estimation accuracy and precision on synthesized FBM datasets. The performance of a maximum likelihood estimator for H, theoretically the best possible estimator, are presented for reference. Of the regression-based methods, it is found that the estimates provided by the DWT method have better accuracy and precision for $H > 0.5$, but become biased for low values of H. The DA method is most accurate for $H < 0.5$ for a 256-point data window size. The PSD method was biased for both $H < 0.5$ and $H > 0.5$.

Keywords—Fractals, Wavelets, Fractional Brownian motion, Dispersional analysis, Heart rate variability

INTRODUCTION

Fractal models have found wide acceptance in many fields of science. They provide a powerful tool for the study of systems that demonstrate long-term correlations and $1/f$-type spectral behavior. The same properties that make fractals powerful models are those that also complicate analysis, however. The extended correlation structure is difficult to capture with standard techniques (*e.g.*, finite-order Autoregressive Moving Average (ARMA) models), and frequency domain analysis is complicated by the nonstationary character of many fractal processes (4,13).

Nevertheless, a model known as fractional Brownian motion (FBM) has provided a mathematical framework for the development of analytical methods appropriate for such processes. Fractional Brownian motion is a nonstationary random process that has infinitely long-run correlations and demonstrates $1/f$-type spectral behavior. FBM also has the interesting property of statistical self-similarity, obeying the relationship:

$$\text{var}[B(t_2, H) - B(t_1, H)] \propto |t_2 - t_1|^{2H} \qquad (1)$$

where $B(t)$ is the FBM process, and H is the Hurst exponent, a single parameter that characterizes the scaling relationship. In this sense, FBM is fractal; it possesses no characteristic time scale, and any selected segment properly rescaled is statistically equivalent to the original process.

The FBM model has been successfully applied in many fields of science, including physiology. FBM models have been proposed for signals such as the electroencephalogram (EEG), heart rate variability (HRV), and regional coronary flow distributions (2,16). Typically a FBM model will be tentatively proposed for such processes based on demonstrated $1/f$-type spectral behavior, and the problem is then to estimate H for the process. In this study, we test a number of estimators for H on simulated data sets to gauge their suitability for biomedical signal processing. We seek to identify accurate estimators that perform well for short data records and limited processing time—two characteristics that are essential in the context of real-time processing of physiological signals.

We begin by reviewing the FBM model, and the process obtained by calculating the increments of FBM, discrete fractional Gaussian noise. We then review three estimators for H. These estimators, based upon the power spectral density (PSD), dispersional analysis (DA), and the discrete wavelet transform (DWT), are alike in that they employ regression analysis to calculate H from basic scaling laws for FBM. They differ, however, in the mathematical domain used to characterize the scaling behavior. We compare the accuracy and precision of the estimators on synthesized FBM data sets of limited size, and compare the results to a maximum likelihood estimator (MLE) for H. The MLE is often considered the best possible estimator and has the desirable properties of being asymptotically unbiased and efficient. The method is computationally intensive, however, and is not well suited for real-time processing. In this study the MLE is used as a

Address correspondence to Dr. Metin Akay, Biomedical Engineering Department, Rutgers University, P.O. Box 909, Piscataway, NJ 08855.
(*Received 12Oct95, Revised 17Jan96, Accepted 13Feb96*)

reference method to show how well H could be estimated, given sufficient processing time.

The FBM Model

The FBM model can be understood as a generalization of Brownian motion. In fact, Mandelbrot and Van Ness (15) define FBM as a moving average of the increments of Brownian motion. Empirical evidence for the presence of a FBM process is often obtained by examination of a given data set in the frequency domain. A FBM process will demonstrate $1/f$-type behavior in the frequency domain over a few orders of magnitude. Alternatively, a number of statistical tests can be performed to determine the suitability of the model (3).

Assuming a FBM model is appropriate, we typically obtain a vector of discrete samples of the process, a discrete fractional Brownian motion (DFBM):

$$B[k,H] = B(k * T_s, H), \quad k = 1,2,3, \ldots, N \tag{2}$$

where $B[k,H]$ is a sampled version of the continuous FBM $B(t,H)$, parameterized by the Hurst exponent H with sampling period Ts.

DFBM, like FBM, is a nonstationary process. However, if we calculate the increments of DFBM,

$$B'[k,H] = B[k,h] - B[k - 1,H], \tag{3}$$

we obtain a result known as discrete fractional Gaussian noise (DFGN). DFGN is a strict sense stationary process that is zero-mean, with Gaussian distribution. The variance of DFGN obeys the scaling relationship in Eq. 1.

METHODS

PSD Method

The relationship between the parameter H and the power spectral density (PSD) of a FBM process has often been exploited to determine H from experimental data. There is no generally accepted definition of the PSD for nonstationary processes, however, so this type of analysis requires further consideration. The nonstationary aspect of FBM implies that the variance and the PSD will be time dependent. In Mandelbrot and Van Ness's work, it is proposed that the nonstationarity can be dealt with by calculating the increments of the process (DFGN) to create a stationary process that is better suited to analysis. However, many researchers have measured the PSD of FBM processes to find that the slope of the PSD is quite consistent, regardless of the position of the observation window. The apparent contradiction was explained by Keshner (11), who showed that when the observation window for such a process is short compared to the total elapsed time since the start of the process, the PSD will maintain the $1/f$-type shape, although the amplitude of the PSD may vary.

Assuming that we are analyzing a trace of FBM that is very short relative to the total elapsed time of the process (the typical case), there are then two viable options for determination of H via the PSD: application of the PSD to the process directly, or to the increments of the process. In the first case the slope of the PSD will be $(-2H - 1)$, in the second case $(1 - 2H)$. In this study we found that the estimates of H obtained by analysis of DFGN were biased in a nonlinear manner, and better results could be obtained by direct analysis of FBM. Accordingly, this is the approach that was adopted for the results presented in this study.

The analysis was implemented as follows:

1. The data vector $x[n]$, $n = 1,2, \ldots, N$ was scaled to unit variance, where $N = 2^M$.

2. The data vector was then divided into two nonoverlapping segments, and a Welch data window was applied to each. A periodogram estimate of the PSD was then calculated for each segment. The two periodogram estimates of power were then averaged at the 2^{M-2} discrete frequencies to form the final estimate. A linear regression analysis was performed on the averaged periodogram to find its slope., taking log(frequency) as the abscissa and log(power) as the ordinate. The estimate of H is calculated from this slope, $H = (\text{slope} + 1)/(-2)$.

Wavelet Method

An essential characteristic of the wavelet transform is the ability to analyze a process relative to scale or resolution. Thus the wavelet transform is uniquely well suited to the analysis of FBM, which is essentially a scale-invariant process. Flandrin demonstrated how FBM, nonstationary in the time domain, could be rendered stationary in the wavelet domain and more amenable to analysis (8).

Given a continuous input signal $x(t)$, the continuous wavelet transform (CWT) can be defined as

$$X_{\text{CWT}}(a,b) = \int x(\gamma)\psi^*_{a,b}(\gamma)d\gamma \tag{4}$$

where * denotes complex conjugation, a represents the scaling factor, and b represents the time.

$\psi_{a,b}(t)$ is obtained by scaling the prototype wavelet $\psi(t)$ at time b and scale a so that

$$\psi_{a,b}(t) = \frac{1}{\sqrt{|a|}}\psi\left(\frac{t-b}{a}\right), \tag{5}$$

for $a,b \in R^+$. Note that R^+ represents the real numbers (1,5,14).

The wavelet transform can be understood by drawing some analogies to the Fourier transform. Both transforms map the input data from the time domain to a new domain in which the data are represented as a weighted sum of

characteristic basis functions. For the Fourier transform, the basis functions are sines and cosines. For the wavelet transform the basis is composed of scaled and shifted versions of a single function, the analyzing or "mother" wavelet, $\psi(t)$ (1,5,14).

The discrete wavelet transform can be obtained by discretizing the parameters a and b. One possible way to do so is to sample the time-scale parameters on a "dyadic" grid (basis 2) in the time-scale plane for the wavelet and scaling parameters. Then,

$$\psi_{j,k}(n) = 2^{\frac{-j}{2}} \psi(2^{-j}n - k), \tag{6}$$

where $j \in Z$, $k \in Z$, $a = 2^j$, $b = k2^j$ and 2^{-j} represents the resolution. Note that the parameter Z represents the set of integers. The discrete parameter j controls the dilation or compression of the scaling and wavelet functions. On the other hand, the parameter k controls the translation in time.

Given a discrete signal $x(n)$, $n \in Z$, its discrete wavelet transform up to a level J of depth (its multiresolution decomposition on J octaves) is defined as

$$x(n) = \sum_{j=1}^{J} \sum_{k \in Z} d_j(k)\psi_{2^j}(n - 2^j k) + \sum_{k \in Z} a_J(k)\phi_{2^J}(n - 2^J k), \tag{7}$$

where $\psi_{2^j}(n - 2^j k)$ are the analysis wavelets and $\phi_{2^J}(n - 2^J k)$ are the scaling sequences. These are the discrete versions of the continuous wavelet: $\psi_{2^j}(t - 2^j k)$ and the scaling function $\phi_{2^J}(t - 2^J k)$; $d_{2^j}(k)$ are the wavelet coefficients, or the detailed signals at scale 2^j; and $a_{2^J}(k)$ are the scaling coefficients, or the approximated signal at scale 2^J.

The work of Mallat (14) led to an efficient algorithm for wavelet decomposition of a discrete signal, and a framework for understanding the wavelet transform in terms of a multiresolution analysis. The algorithm, called the discrete wavelet transform, utilizes a pyramidal algorithm to recursively decompose the signal into approximation and detail signals at successive resolutions.

Let $x(n) = a_{2^0}(n)$ at level $j = 0$. We recursively calculate approximation coefficients $a_{2^{j+1}}(n)$ and detail coefficients $d_{2^{j+1}}(n)$ at lower (coarser) resolutions $j > 0$ via

$$a_{2^{j+1}}(n) = \sum_k g[k - 2n]a_{2^j}(k) = g(n) * a_{2^j}(n) \tag{8}$$

$$d_{2^{j+1}}(n) = \sum_k h[k - 2n]a_{2^j}(k) = h(n) * a_{2^j}(n). \tag{9}$$

Then we keep every other sample of the outcome of the convolution processes (downsampling).

For each decrease in resolution $j + 1$, the representation provides a lower resolution approximation of the signal $a_{2^{j+1}}(n)$ and a detail signal $d_{2^{j+1}}(n)$ equivalent to the difference in information between two successive resolutions. The filters $g[n]$ and $h[n]$ are quadrature mirror filters, respectively, a low-pass and high-pass, that possess impulse responses with the relationship

$$h[n] = (-1)^n g[1 - n]. \tag{10}$$

The quadrature filters are derived for a given wavelet basis and provide the linkage between the multiresolution analysis and the wavelet transform. In this study, the class of compactly supported wavelets proposed by Daubechies (5) was used, satisfying an approximation condition of order 40. The border effect encountered as the transform is applied was handled by imposing periodic ("wrap-around") conditions on the data vector.

For an input signal of length $N = 2^r$, the discrete wavelet transform produces a series of $r - 1$ detail signals of length $N/(2^j)$. The detail signals obey the following scaling relationship for their variance (20):

$$\text{var}[d_{2^j}(n)] = \sigma^2 2^{-(2H+1)j}. \tag{11}$$

Essentially the DWT acts as a whitening filter for FBM such that the $d_{2^j}(n)$ coefficients are rendered weakly correlated in scale and time. Kaplan and Kuo (10) improved the analytical approach by recognizing that the nonstationarity present in FBM can propagate through the recursive calculation used by the DWT to calculate the detail coefficients, and bias the variance progression. They demonstrated that a lower-bias result could be obtained by applying the DWT to DFGN instead of FBM, and our work supports that conclusion. For analysis of DFGN, the scaling relationship is changed to

$$\text{var}(d_{2^j}(n)) = 2^{(2H-1)(j-1)}\sigma^2(2 - 2^{2H-1}), \tag{12}$$

which can be simplified as follows:

$$log_2[\text{var}(d_{2^j}(n)] = (2H - 1)j + f(H,\sigma). \tag{13}$$

In Kaplan and Kuo's work a maximum likelihood estimator developed by Wornell (20) was used to find H based on the variance progression (13). An estimate-maximize (EM) algorithm was then used to search for the ML value of H. To improve the speed of calculation we used the formulation in Eq. 13 directly, and found H by performing a linear regression on a $\log_2$ plot of the detail variance *versus* the resolution level. By calculating H in this manner, we are no longer assured of the desirable properties attributed to the ML method, *i.e.*, asymptotically unbiased and efficient. However, the method is more directly comparable to the PSD and dispersional methods, both of which employ regression analysis, and the method is better suited to real-time processing.

An additional implementational note concerns the exclusion of detail signals. It was empirically found in this study that the accuracy and precision of the wavelet method significantly improved upon exclusion of the first detail signal from analysis; accordingly, the first detail signal was omitted from the regression calculation of H for all results presented in this study. The first detail signal calculated by the wavelet transform is essentially the result of a bandpass filtering operation in which only the highest frequencies of the input are preserved. Our empirical finding may indicate that the data sets analyzed for this study approach white noise at higher frequencies.

Dispersional Analysis

Dispersional analysis, developed by Bassingthwaighte and Raymond (2), estimates the Hurst exponent by assessing the variance or standard deviation of a DFGN process at a succession of resolutions (2). Although this method was developed independently of the wavelet method, it is interesting to note some parallels in the analytical procedure. Like the wavelet method, dispersional analysis calculates H via a variance scaling law that is maintained over a multiresolution decomposition of DFGN. The methods differ in the details of the multiresolution analysis. Dispersional analysis uses a succession of lower-resolution approximations that are obtained by time domain smoothing of the original signal, whereas the wavelet-based method utilizes differences between approximations ("details") obtained via the wavelet transform.

As before, we are considering discretely sampled FBM, the increments are found in Eqs. 2 and 3, and we require the input vector length to be a power of 2. For the implementation utilized in this study, the increments were scaled to unit variance. The algorithm then proceeds as follows:

1. Calculate the sample standard deviation of the vector of increments, SD(1).

2. Form a lower resolution version of the data vector with half as many values by binning adjacent pairs of samples, and replacing them with the means of the pairs. Calculate the sample standard deviation for this lower resolution vector, SD(m), where m is now the number of original vector elements embodied by each element of the lower resolution vector (1,2,4, *etc.*).

3. Repeat step 2, calculating the standard deviation at successively lower resolutions until the vector is reduced to length = 4.

The estimate of H is then calculated by determining the slope of a $\log_{10}$ plot of SD(m) *versus* m as H = slope + 1.

FBM Generation

To compare the analytical methods, it is necessary to have a generative algorithm that can produce traces of FBM with a desired Hurst exponent. A number of algorithms have been proposed (7,13,19). In this study, a generative algorithm developed by Lundahl *et al.* (13) was used. The algorithm uses a Cholesky decomposition of the covariance matrix for DFGN to create a transform that generates DFGN from Gaussian noise. The samples thus produced have the proper correlation structure and long-range dependencies. FBM may then be obtained by discrete integration of the samples.

RESULTS

To assess the accuracy and precision of the estimators, 128- and 256-point FBM datasets for H = 0.05, 0.2, 0.4, 0.6, 0.8, 0.95 were generated with the Cholesky method. Twenty traces of FBM were created at each H level. The mean and standard deviation of the H estimates produced by the three regression-based analysis methods are listed in Table 1 and are shown graphically in Fig. 1. In Fig. 1d the estimates produced by the maximum likelihood estimator for 128-point data sets are shown for reference. These results represent the best-case estimates that could be attained, given sufficient processing time.

It is interesting to compare the wavelet, dispersive, and PSD methods. These methods all use regression calculations to determine H from a fundamental scaling relationship, and are similar in terms of computational load. The wavelet estimator tended to be biased low for low values of H, and became increasingly accurate as H increased. The accuracy and bias were nearly invariant as the data window size was increased from 128 to 256. In contrast, the dispersional analysis estimator was more accurate for

TABLE 1. Mean of H_{EST} and (STD) based on 20 traces of FBM

	128-point traces				256-point traces		
True H	MLE	Wavelet	Dispersive	PSD	Wavelet	Dispersive	PSD
0.05	0.05 (0.01)	−0.26 (0.09)	−0.06 (0.05)	−0.14 (0.08)	−0.19 (0.05)	0.03 (0.05)	−0.19 (0.06)
0.20	0.19 (0.02)	0.04 (0.08)	0.12 (0.04)	0.05 (0.09)	0.10 (0.06)	0.17 (0.05)	0.08 (0.04)
0.40	0.39 (0.02)	0.34 (0.06)	0.33 (0.04)	0.34 (0.09)	0.36 (0.06)	0.36 (0.06)	0.37 (0.05)
0.60	0.58 (0.03)	0.59 (0.04)	0.51 (0.05)	0.63 (0.10)	0.59 (0.05)	0.56 (0.04)	0.65 (0.05)
0.80	0.77 (0.03)	0.81 (0.04)	0.65 (0.06)	1.00 (0.10)	0.81 (0.05)	0.71 (0.04)	0.95 (0.07)
0.95	0.93 (0.02)	0.95 (0.05)	0.72 (0.05)	1.37 (0.11)	0.97 (0.05)	0.82 (0.03)	1.24 (0.08)

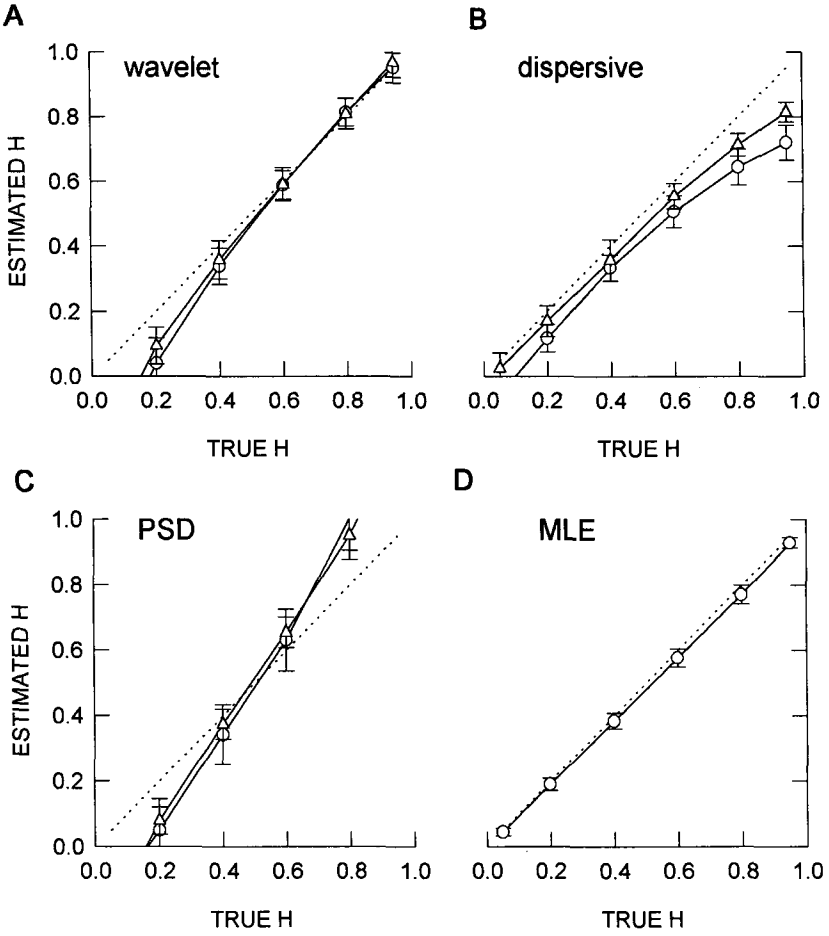

FIGURE 1. Accuracy and variability of four different estimators of *H*. (A) discrete wavelet transform method, (B) dispersional analysis method, (C) power spectral density method, (D) maximum likelihood estimation. Circular data markers indicate estimates calculated for 128-point data sets, triangular markers are estimates for 256-point data sets. The dotted line indicates the true value of *H* used to generate the data sets, and the lengths of the error bars are equivalent to the sample standard deviations for 20 estimates of *H*.

$H < 0.5$, and showed a marked improvement in accuracy as the data window size increased from 128 to 256.

The magnitude and direction of bias for the DA estimator at high H are qualitatively in agreement with an experiment performed by Bassingthwaighte and Raymond (2); however, the bias we observed at $H < 0.5$ contradicts that study, in which a positive bias was observed. The contradiction is likely to be attributable to a difference in the algorithms used to generated the synthesized FBM.

The PSD estimator was biased for $H < 0.5$ and $H > 0.5$ for both the 128- and 256-point data sets, which would impair its usefulness for most applications. A variant of this method was used (17) on larger data sets (512 points and larger) and found to be highly accurate for values of H from 0.1 to 0.9, and superior to the dispersive method. Again, the discrepancy may be due to the FBM generation method used in the study, which was an inverse-PSD technique.

DISCUSSION

It is hoped that the results presented in this study can be used to select appropriate analysis methods for FBM. In particular, the results can be used to compare more recently developed techniques (the wavelet method) to existing approaches. Clearly, we find that the MLE method yields the best estimates for small data set size, regardless of the value of H. The computations required for the ML estimate preclude its use in a real-time application however. The other methods demonstrate performance that is dependent on H, which, of course, would not be known *a priori* in typical use. However, some insight could be obtained by an investigation of the autocorrelation structure of the increments for an unknown process. If a positive autocorrelation ($H > 0.5$) were observed, the wavelet method would be preferred; otherwise the dispersive method would be.

Although we observed clear differences between the various estimators on simulated data sets, a fair question is whether similar performance would be observed with real data sets. To address this issue, we examined a 4-hr segment of HRV data (obtained from a 58-year-old female subject via Holter monitor) by analyzing successive 128-point data windows over the complete segment. A number of authors have observed that HRV contains a strong $1/f$-type component (12,16,21), if so, we would expect estimations of H somewhere in a $0 < H < 0.5$ range. The results are shown in Fig. 2. Although there is no way to know the "true" value of H for this data set, it is interesting to compare the performance of the estimators. In

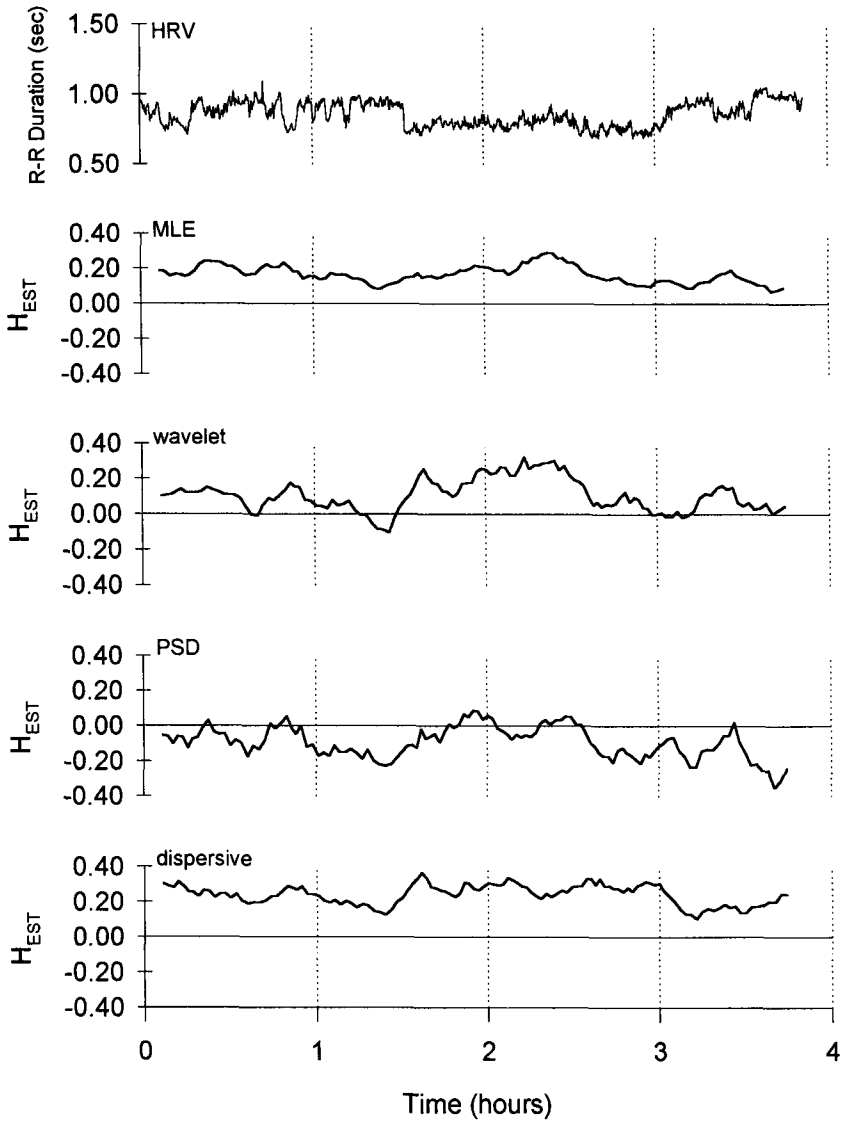

FIGURE 2. Analysis of heart rate variability (HRV) data. The upper plot shows the variability in R-R interval duration over approximately 4 hr. The lower plots show the corresponding estimates of *H* for the MLE, wavelet, PSD, and dispersive analysis methods respectively.

terms of the estimation variance, the results appear to qualitatively concur with the simulation study: lowest variance for the MLE method, greatest variance for the PSD method, with the other methods somewhere in between. It is difficult to assess the accuracy of the H estimates for the different methods without foreknowledge of H; however, we observe that the bias of the estimates relative to each another is what we would qualitatively expect based on the simulation study.

The accuracy and precision of the estimates generated by the MLE method are great enough to lead one to ask whether it would be possible to lower the inherent computational load in some manner. The computational delays are attributable to two sources. One is the search of the likelihood function for its maximum value, the other is the calculation of the log-likelihood value itself as the search proceeds. It may be possible to construct a hybrid estimator in which the initial estimate of H is generated by a regression-based method such as the dispersional or wavelet methods, and then to employ the MLE method for what should be a short search for the ML value of H. The computational requirements would then be dominated by the calculation of the ML estimate rather than the search process. This could potentially lower the computational load suffciently to allow real-time estimation.

Another outstanding issue is the performance of the estimators in noise. Lundahl (13) showed that the accuracy of the ML estimates can degrade severely in the presence of noise at a 30-dB SNR level. For noisy data sets, the MLE would need to be redefined to model the expected noise source. Wavelet-based estimators have been presented (10,20) that use ML techniques to estimate H for data sets contaminated by Gaussian noise. These methods were still found to be unreliable for short noise-contaminated data sets, however. Further work is needed in this area.

REFERENCES

1. Akay, M. Wavelets in biomedical engineering. *Ann. Biomed. Eng.* 23:531–542, 1995.
2. Bassingthwaighte, J. B., and G. M. Raymond. Evaluation of the dispersional analysis method for fractal time series. *Ann. Biomed. Eng.* 23:491–505, 1995.
3. Beran, J. Statistical methods for data with long-range dependence. *Statistical Sci.* 7:404–427, 1992.
4. Christini, D. J., A. Kulkarni, S. Rao, E. R. Stutman, F. M. Bennett, J. M. Hausdorff, N. Oriol, and K. R. Lutchen. Influence of autoregressive model parameter uncertainty on spectral estimates of heart rate dynamics. ABME 23:127–134, 1995.
5. Daubechies, I. Orthonormal bases of compactly supported wavelets. *Comm. Pure Appl. Math.* 44:909–996, 1988.
6. DeBoer, R. W., J. M. Karemaker, and J. Strackee. Comparing spectra of a series of point events particularly for heart rate variability data. *IEEE Trans. Biomed. Eng.* BME-31:384–387, 1984.
7. Feder, J. Fractals. New York: Plenum Press, 1988, 310 pp.
8. Flandrin, P. On the spectrum of fractional Brownian motion. *IEEE Trans. Inform. Theor.* 35:197–199, 1989.
9. Flandrin, P. Wavelet analysis and synthesis of fractional Brownian motion. *IEEE Trans. Inform. Theor.* 38:910–917, 1992.
10. Kaplan, L. M., and C. C. Jay Kuo. Fractal estimation from noisy data via discrete fractional Gaussian noise (DFGN) and the Haar basis. *IEEE Trans. Signal Proc.* 41:3554–3562, 1993.
11. Keshner, M. S. $1/f$ noise. *Proc. IEEE* 70:212–218, 1982.
12. Kobayashi, M., and T. Musha. $1/f$ fluctuation of heartbeat period. *IEEE Trans. Biomed. Eng.* BME-29:456–457, 1982.
13. Lundahl, T., W. J. Ohley, S. M. Kay, and R. Siffert. Fractional Brownian motion: A maximum likelihood estimator and and its application to image texture. *IEEE Trans. Med. Imag.* MI-5:152–161, 1986.
14. Mallat, S. G. A theory for multiresolution signal decomposition: The wavelet representation. *IEEE Trans. PAMI* 11: 674–693, 1989.
15. Mandelbrot, B. B., and J. W. Van Ness. Fractional Brownian motions, fractional noises and applications. *SIAM Rev.* 10:422–437, 1968.
16. Saul, J. P., P. Albrecht, R. D. Berger, and R. J. Cohen. Analysis of long term heart rate variability: Methods, $1/f$ scaling and implications. *Comp. Cardiol.* 14:419–422, 1987.
17. Schepers, H. E., J. H. G. M. van Beeck, and J. B. Bassingthwaighte. Four methods to estimate the fractal dimension from self-affine signals. *IEEE Eng. Med. Biol. Magazine.* 11 (June):57–64, 1992.
18. Tewfik, A. H., and M. Kim. Correlation structure of discrete wavelet coefficients of fractional Brownian motion. *IEEE Trans. Inform. Theor.* 38:904–909, 1992.
19. Voss, R. F. Fractals in nature: From characterization to simulation. In: The Science of Fractal Images, edited by H. O. Peitgen and D. Saupe. New York: Springer-Verlag, 1988, pp. 21–70.
20. Wornell, G. W., and A. V. Oppenheim. Estimation of fractal signals from noisy measurements using wavelets. *IEEE Trans. Signal Proc.* 40:611–623, 1992.
21. Yamamoto, Y., and R. L. Hughson. Coarse-graining spectral analysis: New method for studying heart rate variability. *J. Appl. Physiol.* 71:1143–1150, 1991.